Available online at www.sciencedirect.com
ScienceDirect
Polymer 49 (2008) 836–842
polymer
www.elsevier.com/locate/polymer

Polymer Communication

Peculiar dynamics and elastic properties of hybrid semi-interpenetrating polymer network–3-D diamond nanocomposites

Vladimir Bershtein [a,*], Lyudmyla Karabanova [b], Tatiana Sukhanova [c], Pavel Yakushev [a], Larisa Egorova [a], Elena Lutsyk [b], Anna Svyatyna [b], Milana Vylegzhanina [c]

[a] *Ioffe Physico-Technical Institute, Russian Academy of Sciences, 194021 St. Petersburg, Russia*
[b] *Institute of Macromolecular Chemistry, National Academy of Sciences of Ukraine, 02660 Kyiv, Ukraine*
[c] *Institute of Macromolecular Compounds, Russian Academy of Sciences, 199004 St. Petersburg, Russia*

Received 18 December 2007; accepted 4 January 2008
Available online 6 January 2008

Abstract

Polyurethane–poly(2-hydroxyethyl methacrylate)-3-D nanodiamond (PU–PHEMA–ND) composites were studied using combined CRS/DSC/AFM approach. The peculiar behavior and the pronounced heterogeneity of their glass transition dynamics were revealed. Two opposite tendencies for changing dynamics by 3-D NDs, with prevailing sharp suppression of motions, and three-fold increasing elastic properties were shown. Maximal effects were found at minimal ND content of 0.25 wt%. This was associated, besides the improved dispersion/spatial distribution of NDs, with formation of thoroughly cross-linked nanocomposite network, due to the double hybridization resulting in a low rheological percolation threshold and the synergistic effect in dynamics.

Keywords: Interpenetrating polymer networks; Diamond nanocomposites; Dynamics

1. Introduction

Polymer composites, containing small additives of nanofillers, attracted great attention last decade, both in industry and academician studies, since a considerable enhancement of mechanical, thermal and other properties may be attained in these materials compared with those of virgin polymers. To date, most studies have focused on polymer nanocomposites containing 2-D silicate nanolayers [1,2] or 1-D carbon nanotubes (CNTs) [3–5]. The key to their enhanced efficiency is achieving a good dispersion, uniform spatial distribution and alignment (for CNTs) of nanoparticles. In addition, the critical role of two other points is typically emphasized, viz., (a) a high aspect ratio (e.g., length-to-diameter for CNTs) for a nanofiller, and (b) the necessity of a special chemical functionalization of nanofiller surface to provide its covalent coupling with a polymer matrix. The points (a) and (b) are typically considered as the important prerequisites for attaining the highest performance of a polymer nanocomposite, in particular a low "percolation rheological threshold" (distinct effect of improved rheological behavior) at nanofiller content of less than 1 wt% [6,7]. The peculiarities of segmental dynamics in nanocomposites are currently studied experimentally (basically for composites with 1-D and 2-D nanofillers) and discussed in the context of polymers located in confined nanospaces and manifesting a special dynamic behavior [5,8–20].

Among nanocarbon structures, widely utilized in recent years as polymer nanofillers (CNTs, nanorods, nanofibers, fullerenes, nanodiamonds (NDs)) [3–5,21], only NDs have been available on a relatively large scale for last two decades [4]. There are the examples of their successful applications in polymer nanocomposites as electronics materials [22]; materials with protonic conductivity [23] or enhanced thermal conductivity [24]; in selective membranes, sensors, catalytic systems, nonlinear optical materials [21,25], and as the

* Corresponding author. Tel.: +7 812 2927172; fax: +7 812 2971017.
E-mail address: vbersht@polmater.ioffe.ru (V. Bershtein).

0032-3861/$ - see front matter © 2008 Elsevier Ltd. All rights reserved.
doi:10.1016/j.polymer.2008.01.002

nanofillers increasing strength, wear and heat-ageing resistance of elastomers [4,21,26,27].

In the previous work [28] we studied dynamics of PU–PHEMA semi-IPNs using laser-interferometric creep rate spectroscopy/differential scanning calorimetry (CRS/DSC) analysis. These two-phase materials [29] demonstrated the pronounced dynamic heterogeneity within the extraordinarily broadened PHEMA and PU glass transitions. In fact, the united glass transition in the temperature range from −60 °C to 160 °C was observed in these networks. Such anomalous dynamics plus their improved biocompatibility [30] are of interest for the development of improved biomedical, damping or membrane materials based thereon.

In the present research we revealed a possibility of large and specific impact of low 3-D nanofiller content, without performing a special functionalization of its surface, on glass transition dynamics and the elastic properties of polymer matrix. This was shown for the nanocomposites based on PU–PHEMA semi-IPNs doped with 3-D nanodiamonds.

2. Experimental section

2.1. Materials

The PU–PHEMA networks were prepared as described elsewhere [28,31]. First, PU network was obtained from the adduct of trimethylol propane and toluylene diisocyanate, and poly(oxypropylene)glycol (PPG) with $M_w = 2.000\ g\ mol^{-1}$. Semi-IPNs were prepared by swelling PU with 2-hydroxyethyl methacrylate (HEMA) and its subsequent photopolymerization (the wavelength of UV light $\lambda = 340$ nm). This communication shows the effects observed for the nanocomposites with PU–PHEMA weight ratio of 83/17. The diamond powder, obtained by the shock-wave method (supplied by Alit, Ukraine), with particle sizes of 2–100 nm and specific surface area of $220\ m^2\ g^{-1}$, was introduced in the amounts of 0.25, 1 or 3 wt% into the matrix at the stage of PU synthesis. NDs were dried for 48 h at 200 °C before using. The prepared films with 1 mm thickness were postcured for 2 h at 100 °C and then were held for 36 h at 80 °C in vacuum (10^{-5} Pa).

2.2. Characterization

CRS, the high-resolution method of relaxation spectrometry and thermal analysis [32–34], was used here for discrete dynamic analysis. It has earlier been applied successfully for studying dynamic heterogeneity in different complex polymer systems [35–38]. CRS setups and the experimental technique have been described in detail elsewhere [32–34]. It consists of precisely measuring creep rates at a low stress as a function of temperature, using a laser interferometer based on the Doppler effect. The time evolution of deformation is registered as a sequence of low-frequency beats in an interferogram whose beat frequency ν yields a creep rate $\varepsilon^* = \lambda\nu/2I_0$, where $\lambda = 630$ nm is a laser wavelength, and I_0 is an initial sample length. The stresses were chosen as capable of inducing sufficient creep rates to be measured, while maintaining also a high spectral resolution, without smoothing and distortion of a spectral contour, and preventing a premature rupture of a sample. The interferometer was used also for determination of tensile "modulus of elasticity" E versus T plots, obtained from the values of 1s deformation $\varepsilon = \lambda n/2I_0$ where n is a number of oscillations in an interferogram. Film samples with $1 \times 5 \times 50\ mm^3$ size were used. Loading of a sample, recording of an interferogram, and unloading were performed upon every 5 °C of heating with the rate of about 1 °C/min.

Perkin–Elmer DSC-2 apparatus was used for characterization of PHEMA glass transition in the neat PHEMA, PU–PHEMA semi-IPNs and the nanocomposites. The second scans were taken in order to exclude the side endothermic effect of water desorption. Deflection atomic force microscopy (AFM) images were obtained in contact mode for estimation of the dispersion/spatial distribution of NDs in the matrix. Nanotop NF-206 apparatus ("Microtestmashiny", Belarus) was utilized.

3. Results and discussion

Fig. 1 shows the DSC curves characterizing PHEMA glass transition in the dehydrated PHEMA, 83PU–17PHEMA network and ND nanocomposites. Only small increase in T_g of PHEMA after its doping with NDs is observed. Contrarily, the large displacement to higher temperatures, with broadening and arising two stages ($T_{g1} = 105$ °C and $T_{g2} = 163$ °C), is observed for the PHEMA glass transition in the 83PU–17PHEMA network, despite much lower T_g for the neat PU network [28,31]. The introduction of NDs into this network results in a total suppression of the higher-temperature transition (heat capacity ΔC_{p2} step), and reduction of ΔC_{p1} step, with its shift by 15–20 °C to lower temperatures. These DSC curves suggest dynamic heterogeneity within the broad PHEMA glass transition in the PU–PHEMA network and substantial modifying dynamics by 3-D ND additives. Really, the creep rate (CR) spectra obtained were consistent with such suppositions.

Fig. 2a shows the CR spectrum of neat PU network in the temperature region of glass transition, between −60 °C and 50 °C. It consists of four overlapping peaks with the maxima at about −30 °C (I), −10 °C (II), 10 °C (III), and 40 °C (IV). Peaks I–III were tentatively assigned to unfreezing different dynamic modes within PPG crosslinks, whereas peak IV was associated with motion of network junctions [28]. The introduction of NDs into the PU network results in some redistribution of the intensities of spectral peaks; NDs affect stronger lower-temperature peaks, suppressing to larger extent motion of segments located at some distance from network junctions (peaks I and II). The introduction of 17 wt% PHEMA into the PU network leads to the pronounced suppression of PU dynamics (Fig. 2a). Qualitatively similar influence of NDs on PU dynamics in the 83PU–17PHEMA networks was observed (the spectra, obtained at 3 MPa, are not given here): basically suppression of creep was registered at −60 °C to −40 °C but its acceleration was observed at the temperatures of −20 °C to 20 °C for the nanocomposites with 1 or 3% NDs.

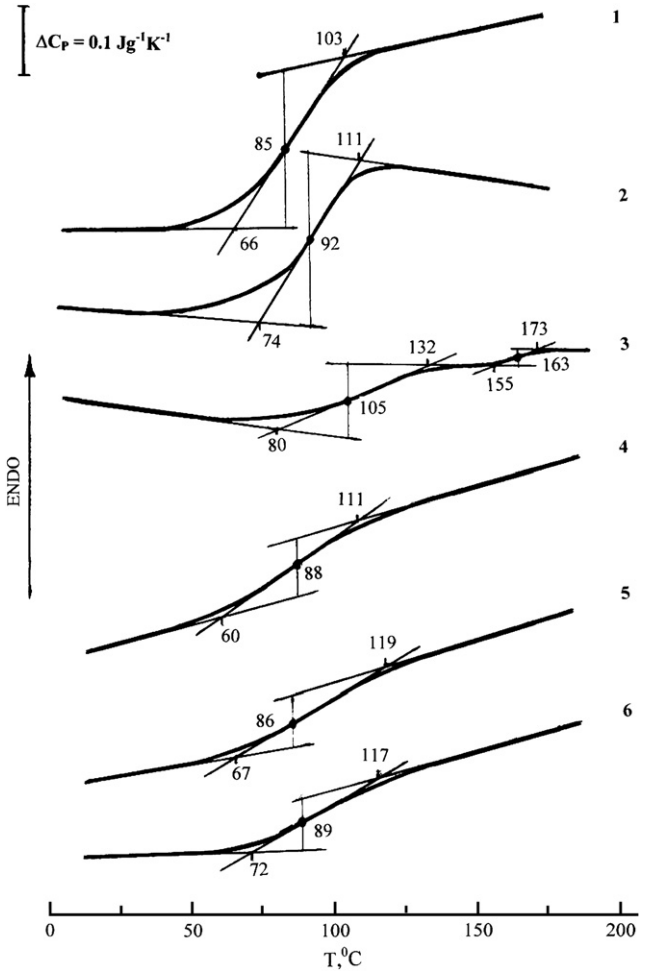

Fig. 1. DSC curves obtained in the region of PHEMA glass transition for neat PHEMA (1); PHEMA with 3% NDs (2); 83PU–17PHEMA semi-IPN (3), and 83PU–17PHEMA–ND nanocomposites with 0.25% (4), 1% (5), and 3 wt% NDs (6). Scans II were taken at the heating rate of 20 °C/min, after heating to 200 °C and subsequent cooling to −20 °C at the rate of 320 °C/min. Glass transition temperature T_g at the half-height of a heat capacity step ΔC_p, the temperatures of the glass transition onset T_g' and completion T_g'', as well as the ΔC_p values are indicated.

Fig. 2b shows a single glass transition peak with $T_{max} = 90$ °C in the spectrum of the neat PHEMA. In the spectrum of the PHEMA–ND composite, its shape changes but without T_{max} shift. In the case of the 83PU–17PHEMA network, a single T_g peak transforms into the complicated contour consisting of several partly overlapping peaks, which are located between 50–70 °C and 160 °C; creep rate sharply accelerates from ca. 170 °C for this network (Fig. 2c).

Fig. 2c shows that doping the 83PU–17PHEMA network with NDs dramatically changes the relaxation picture. The main effect is a sharp suppression of dynamics (creep rate reduction) over the temperature range of 90–180 °C. Consequently, the suppression of creep after the introduction of NDs is much more pronounced in the semi-IPN than that in both pure components. The most evident, largest creep depression at 150–180 °C is observed at the minimal ND content of 0.25 wt% in the nanocomposite. The introduction of ND particles also results in some increase of creep rates at 20–80 °C,

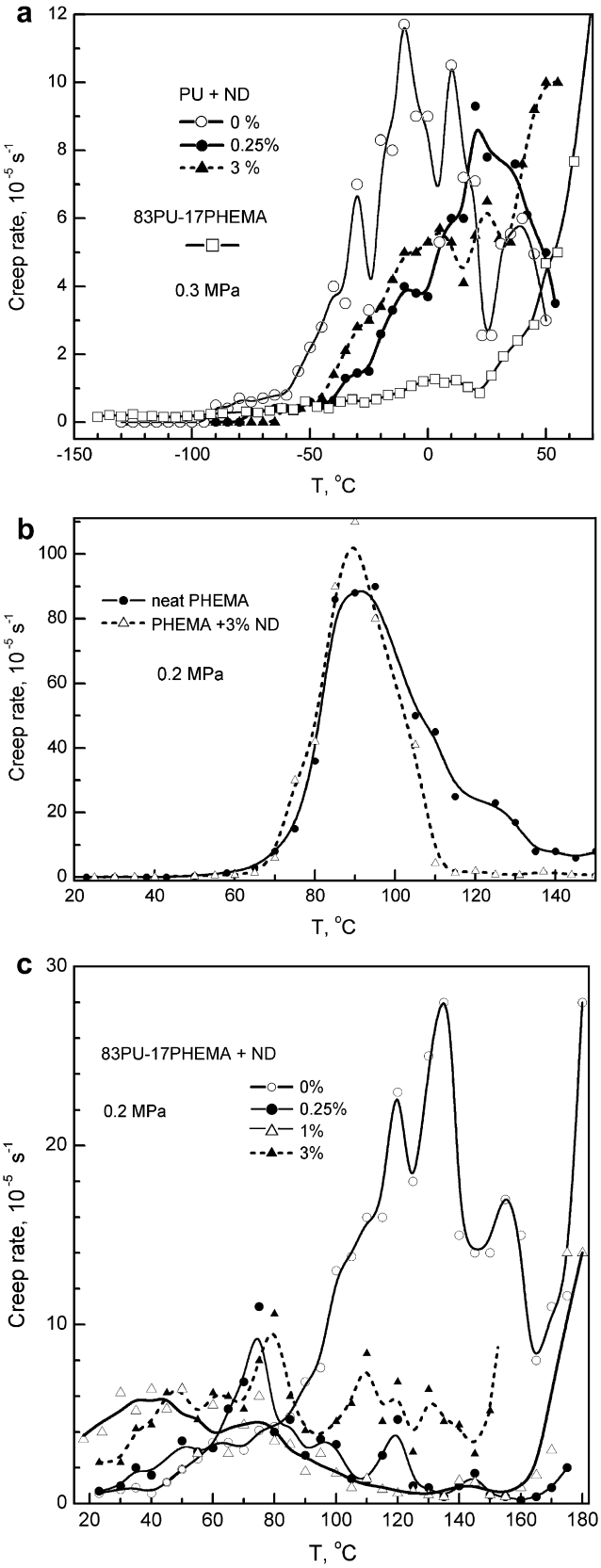

Fig. 2. Creep rate spectra obtained for PU, PHEMA and 83PU–17PHEMA semi-IPN as well as for diamond nanocomposites based thereon, at tensile stresses of 0.3 or 0.2 MPa in the temperature regions of PU (a) and PHEMA (b, c) glass transitions. ND weight contents in the nanocomposites are indicated.

i.e., in the temperature region between the α- and β-transitions of PHEMA. Thus, ND additives modify PHEMA glass transition in the PU–PHEMA networks in two opposite directions; however, suppression of dynamics is much more pronounced.

Similarly, tensile modulus of elasticity E versus temperature plots show a large influence of small ND additives, depending on the ND content in a nanocomposite and a temperature region. Fig. 3 shows that the large effects of the enhancement of rigidity, with E increasing by ca. 300%, are observed in the temperature regions of PHEMA or PU glass transitions. And, again, the maximal increase of a modulus is observed at the minimal ND content of 0.25% in the nanocomposite. Moreover, the introduction of 3% NDs may result even in a large E reduction (Fig. 3b).

We found that the aforementioned anomalies were associated with different ND dispersion/distribution in the matrix and the effect of "double hybridization" in the systems studied, as it is discussed below.

AFM images showed three kinds of ND dispersion/distribution in the 83PU–17PHEMA matrix: as individual nanoparticles of ca.100 nm or less in size (I); their agglomerates with the size of 0.2–0.5 μm (II), and their larger aggregates from 0.6 μm up to several micrometers in size (III) (Fig. 4). Generally, all these dispersion states are revealed in the nanocomposites with 0.25, 1 or 3 wt% NDs, however, they contribute very differently to their structures. For the composite with 0.25% NDs, individual nanoparticles prevail and are relatively uniformly distributed, whereas small ND aggregates are rather sparse (Fig. 4a and b). Dispersion states II and III turned out to be more characteristic of the nanocomposite with 1% NDs, where individual ND particles are less discernable (Fig. 4c and d). At last, the nanocomposite with 3% NDs was characterized not only with the presence of a large quantity of ND agglomerates II and micron aggregates III in the structure, but also with their sharply non-uniform spatial distribution. Thus, comparing Fig. 4e and f shows both microdomains with high concentration of ND aggregates and microdomains practically free from the latters. Besides, a large difference in the ND quantities at two film surfaces was found for the nanocomposite films with 1 or 3 wt% NDs. These data clarify the reason for the largest effects of changing dynamics and modulus just in the nanocomposite with 0.25% NDs, where relatively good dispersion and distribution of nanofiller particles promoted their largest influence on the matrix, due to a maximal interfacial area despite a minimal ND content.

Nevertheless, the large impact of a small additive of 3-D nanofiller, in the absence of a special functionalization of its surface, on polymer matrix is an unexpected and remarkable fact. Really, the calculations [4,5] assume, for 3-D nanofiller, a totally nanoscopically-confined state of a matrix in case an average interparticle distance, L, is close to or less than the unperturbed dimensions of macromolecular random coil, as estimated by radius of gyration R_g, typically of an order of 10 nm in size for many polymers. Meantime, $L > 300–500$ nm $\gg R_g$ in case 1% of 3-D particles of 50–100 nm size are introduced [4,5].

We tried to clarify this problem and found that the effects obtained were associated, obviously, with formation of a specifically cross-linked structure due to "double chemical hybridization".

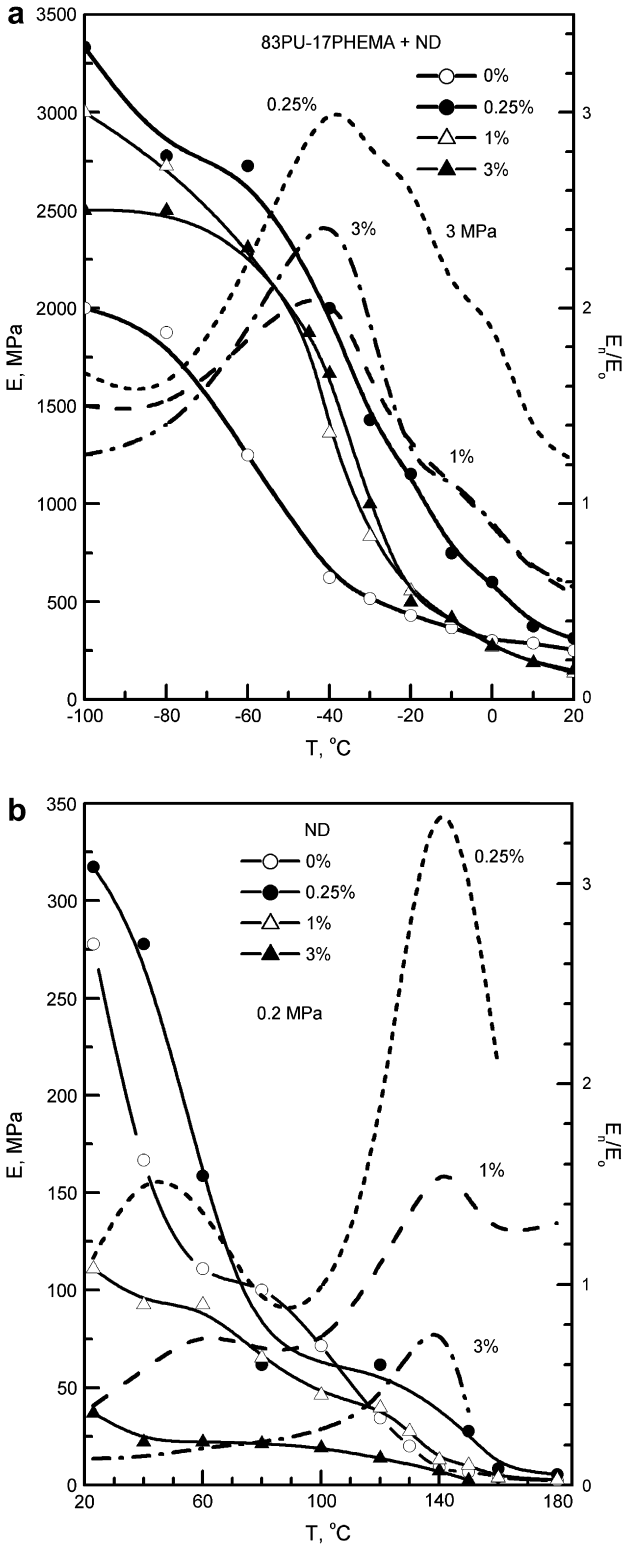

Fig. 3. Tensile modulus of elasticity E versus temperature plots obtained by using a laser interferometer for the 83PU–17PHEMA network (E_0) and its nanocomposites (E_n) in the temperature regions of PU (a) and PHEMA (b) glass transitions. The interrupted lines indicate E_n/E_o ratios.

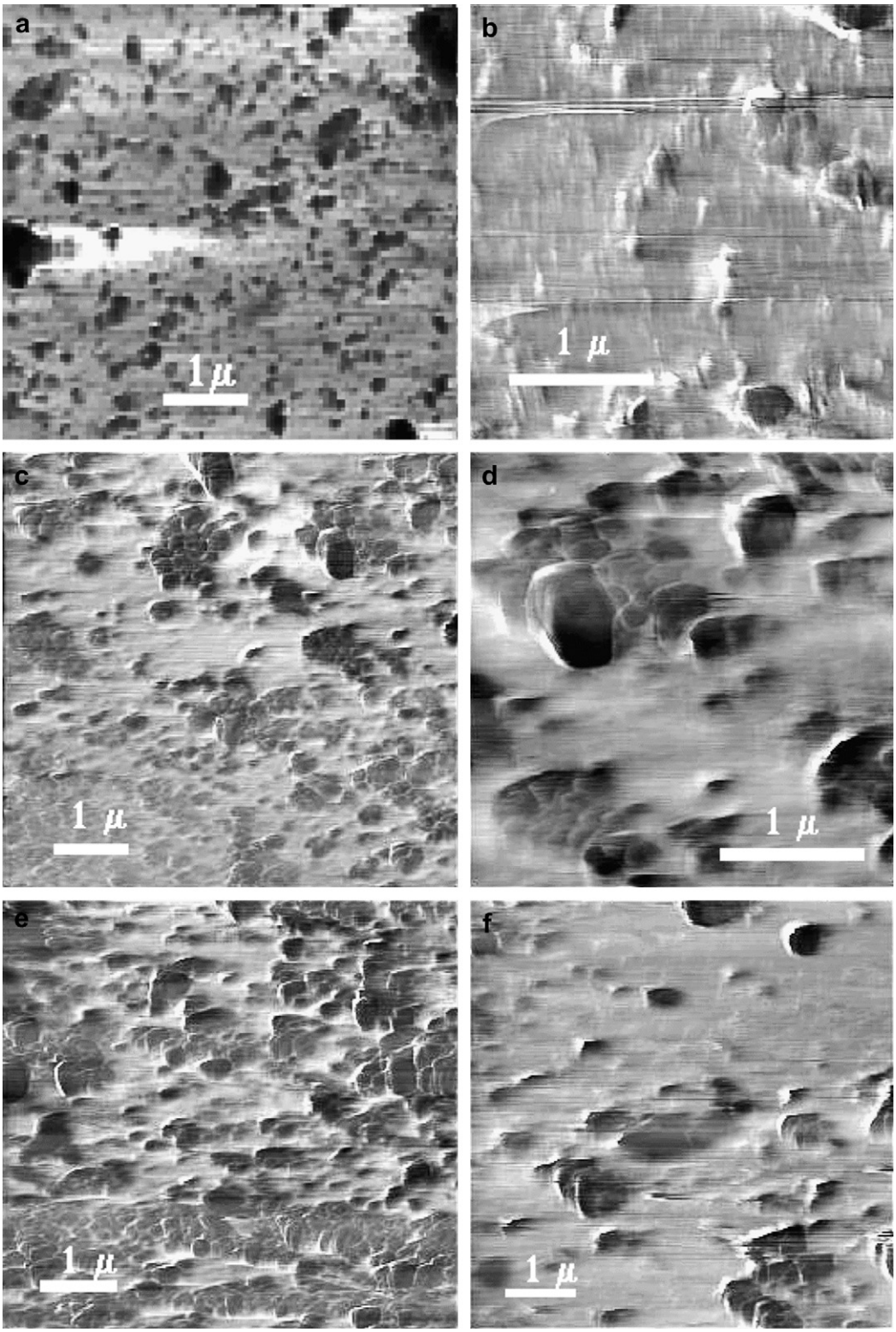

Fig. 4. Deflection AFM images (in contact mode) of the 83PU–17PHEMA–ND nanocomposite films with 0.25 wt% (a, b), 1 wt% (c, d), and 3 wt% NDs (e, f).

First, we found by IR spectroscopy that a very small concentration of unreacted isocyanate groups remained in the PU network, and it sharply decreased after swelling PU network with HEMA monomer and its polymerization, i.e., in the PU–PHEMA network [28]. There is a negligibly small probability that totally ''free'' molecules of the adduct of trimethylol propane and toluylene diisocyanate remain in their liquid mixture with low-molecular-weight PPG, i.e., in the presence of a sufficient concentration of end PPG hydroxyls and highly-reactive isocyanate groups. This allowed us to assume the reaction between HEMA hydroxyls and unreacted isocyanate groups of some of PU junctions occurs, due to

the ''incompleteness'' of these junctions for steric reasons. Grafting PHEMA molecules to PU network junctions, including, perhaps, many-point covalent attaching, may create local hindrances, impeding segmental dynamics, e.g., by preventing conformational (T–G) transitions peculiar to glass transition events, or due to increasing a motional event scale. This may explain, in our opinion, anomalous dynamics in the 83PU–17PHEMA network, in particular, the displacement of PHEMA glass transition to higher temperatures in the presence of low-T_g PU network.

And, secondly, a process of ''self-functionalization'' of ND surface occurred during preparing these nanoparticles. As found spectroscopically [39,40], the surface of ND particles, obtained by a shock-wave method, is chemically-active since it readily acquires a ''functional cover'' (OH, COOH and other groups) after high-temperature drying, before their introduction into the reaction mixture. Then, in view of high reactivity of isocyanate groups towards these groups, the hybridization reaction between isocyanate groups of adduct and a ''functional cover'' of NDs, undoubtedly, occurs during the formation of PU network in the presence of ND particles. As a result, double hybridization in the hybrid PU–PHEMA–ND nanocomposites may be considered as the second important factor for the manifestation of a strong impact of 3-D NDs on the matrix dynamics and elastic properties.

Specific cross-linking exerted, in fact, a ''synergistic effect'' on the PHEMA glass transition dynamics (Fig. 2). Really, adding NDs to the neat PHEMA modified only to small extent its glass transition. PU–PHEMA hybridization resulted in a large displacement of the PHEMA glass transition to higher temperatures and arising the pronounced dynamic heterogeneity. At the same time, the combined influence of PU and small ND additive on PHEMA dynamics in the 83PU–17PHEMA–ND nanocomposite was completely non-additive, providing the strong suppression of dynamics (creep at a small stress) over the 90–180 °C temperature range.

Two opposite tendencies of dynamics/modulus changes in the nanocomposites studied may be treated in terms of constraining dynamics, due to strong interactions between system constituents, and, contrarily, accelerating dynamics in nanoscale-confined geometries, due to decrease, locally, in packing density and motional cooperativity degree Z in the presence of nanofiller particles. We believe that the accelerating effect and its limits can be explained in terms of the common nature of α- and β-relaxations in flexible-chain polymers as intermolecularly cooperative or quasi-independent motions, respectively, in chain sections approximately equal in length to a Kuhn statistical segment [41–43]. Loosened molecular packing in a complex polymer system may lead to decreasing Z that results in the displacement of T_g to lower temperatures. The physical limit for changing dynamics in the such case is ''transformation'' of α-relaxation into β-relaxation, i.e., the glass transition manifests itself as non-cooperative segmental motion ($Z \approx 1$) in the temperature region of β-relaxation; it may be seen, in particular, from Fig. 2c.

It should be mentioned that the complicated, two- or three-, or even four-stage glass transition for one polymer component, with simultaneous manifestation of both increased and decreased T_g values, has been registered at first, probably, for block copolymers [44,45]. A common scheme, illustrating the possible anomalies of glass transition behavior in complex polymer systems, was given in the review [37]. Last years, the special glass transition dynamics has been demonstrated in a number of experiments [8–20] modeling, basically, behavior of polymer matrices in nanocomposites with 2-D silicate nanolayers or 1-D carbon nanotubes.

4. Conclusion

In this research, we demonstrated a large impact of low 3-D nanoparticles content, without performing a special functionalization of their surface, on polymer matrix dynamics and the elastic properties. A low rheological percolation threshold (at 0.25 wt% nanofiller) and the synergistic effect in dynamics were observed for the 3-D diamond-containing nanocomposites based on the PU–PHEMA IPN, despite an average interparticle distance $L \gg R_g$. The peculiar cross-linking in the system, due to the double covalent hybridization, made it possible to observe such an effect which is peculiar usually to composites with 1-D or 2-D nanofillers. The nanocomposites studied behave, to a certain extent, as ''interface controlled materials''.

References

[1] Ray SS, Okamoto M. Prog Polym Sci 2003;28:1539.
[2] Alexandre M, Dubois P. Mater Sci Eng 2000;28:1.
[3] Moniruzzaman M, Winey KI. Macromolecules 2006;39:5194.
[4] Hu Y, Shenderova OA, Hu Z, Padgett CW, Brenner DW. Rep Prog Phys 2006;69:1847.
[5] Shaffer MSP, Sandler JKW. In: Advani S, editor. Processing and properties of nanocomposites. World Sci Publ; 2006.
[6] Du F, Scogna RC, Zhou W, Brand S, Fischer JE, Winey KI. Macromolecules 2004;37:9048.
[7] Hu G, Zhao C, Zhang S, Yang M, Wang Z. Polymer 2006;47:480.
[8] Huwe A, Kremer F, Behrens P, Schweiger W. Phys Rev Lett 1999;82:2338.
[9] Giannelis EP, Krishnamoorti R, Manias E. Adv Polym Sci 1999;138:107.
[10] Anastaisiadis SH, Karatasos K, Viachos G, Manias E, Giannelis EP. Phys Rev Lett 2000;84:915.
[11] Vaia RA, Giannelis EP. MRS Bull 2001;26:394.
[12] Tien YI, Wei KH. J Appl Polym Sci 2002;86:1741.
[13] Bershtein VA, Egorova LM, Yakushev PN, Pissis P, Sysel P, Brozova L. J Polym Sci Part B Polym Phys 2002;40:1056.
[14] Manias E, Kuppa V. Eur Polym J 2002;8:193.
[15] Schonhals A, Goering H, Schick Ch. J Non-Cryst Solids 2002;305:140.
[16] Kuppa V, Manias E. J Chem Phys 2003;118:3421.
[17] Lu H, Nutt S. Macromolecules 2003;36:4010.
[18] Ellison CJ, Torkelson JM. Nat Mater 2003;2:695.
[19] Urbanczyk L, Hrobaricova J, Calber C, Jerome R, Grandjean J. Langmuir 2006;22:4818.
[20] Rittigstein P, Priestley RD, Broadbelt LJ, Torkelson JM. Nat Mater 2007;6:278.
[21] Dolmatov VYu. Russ Chem Rev 2001;70:687.
[22] Dolmatov VYu. In: Shenderova OA, Gruen DM, editors. Ultrananocrystalline diamond: synthesis, properties and applications. Norwich, New York: William-Andrew Publ; 2006.
[23] Williams OA, Zimmermann T, Kubovic M, Denisenko A, Kohn E, Jackman RB, et al. In: Gruen DM, Shenderova OA, Vul' AY, editors.

Synthesis, properties and applications of ultrananocrystalline diamond. Amsterdam: Springer; 2005.
[24] Shilov VV, Gomza YP, Shilova OA, Padalko VI, Efimova LN, Nesin SD. In: Gruen DM, Shenderova OA, Vul' AY, editors. Synthesis, properties and applications of ultrananocrystalline diamond. Amsterdam: Springer; 2005.
[25] Davidson JL, Kang WP. In: Gruen DM, Shenderova OA, Vul' AY, editors. Synthesis, properties and applications of ultrananocrystalline diamond. Amsterdam: Springer; 2005.
[26] Voznyakovskii AP. Phys Solid State 2004;46:644.
[27] Ghosh A, Sciamanna SF, Dahl JE, Shenggao L, Carson MK, Schiraldi DA. J Polym Sci Part B Polym Phys 2007;45:1077.
[28] Karabanova LV, Sergeeva LM, Svyatyna AV, Yakushev PN, Egorova LM, Ryzhov VA, et al. J Polym Sci Part B Polym Phys 2007;45:963.
[29] Shilov VV, Karabanova LV, David L, Boiteux G, Seytre G, Gomza YP, et al. Polimernjy Zh (Ukraine) 2005;27:255.
[30] Karabanova LV, Boiteux G, Seytre G, David L, Stevenson I, Lachenal G, et al. In: Proceedings of the 12th European Conference on Composite Materials, Biarritz, France; 2006.
[31] Karabanova LV, Boiteux G, Gain O, Seytre G, Sergeeva LM, Lutsyk ED. Polym Int 2004;53:2051.
[32] Peschanskaya NN, Yakushev PN, Sinani AB, Bershtein VA. Thermochim Acta 1994;238:429.
[33] Bershtein VA, Yakushev PN, Peschanskaya NN. Macromol Symp 1999;147:73.
[34] Bershtein VA, Yakushev PN, Karabanova LV, Sergeeva LM, Pissis P. J Polym Sci Part B Polym Phys 1999;37:429.
[35] Bershtein VA, David L, Egorov VM, Egorova LM, Yakushev PN, Pissis P, et al. Polymer 2002;43:6943.
[36] Bershtein VA, David L, Egorov VM, Fainleib AM, Grigorieva OP, Bey I, et al. J Polym Sci Part B Polym Phys 2005;43:3261.
[37] Bershtein VA, David L, Egorov VM, Pissis P, Sysel P, Yakushev PN. In: Mittal KL, editor. Polyimides and other high temperature polymers, vol. 3. Utrecht-Boston: VSP; 2005.
[38] Bershtein VA, Egorova LM, Yakushev PN, Sindelar V, Sysel P, Sukhanova TE, et al. Polym Bull 2007;56:65.
[39] Korobko AP, Krasheninnikov SV, Levakova IV, Ozerina LA, Chvalun SN. Polym Sci A 2001;43:1163.
[40] Kulakova II. Phys Solid State 2004;46:636.
[41] Bershtein VA, Egorov VM. Differential scanning calorimetry of polymers: physics, chemistry, analysis, technology. New York: Ellis Horwood; 1994.
[42] Bershtein VA, Egorov VM, Egorova LM, Ryzhov VA. Thermochim Acta 1994;238:41.
[43] Bershtein VA, Ryzhov VA. Adv Polym Sci 1994;114:43.
[44] Bershtein VA, Levin VY, Egorova LM, Egorov VM, Zhdanov AA, Slonimsky GL, et al. Vysokomol Soedin A 1987;29:2360.
[45] Bershtein VA, Levin VY, Egorova LM, Egorov VM, Zhdanov AA, Slonimsky GL, et al. Vysokomol Soedin A 1987;29:2553.